CHAPTER 177

Bed Boundary Layers

B.A. O'Connor[1], J.M. Harris[1], H. Kim[1], Y. K. Wong[1], H.U. Oebius[2], and J.J. Williams[3].

ABSTRACT

The paper describes the development and application to laboratory and North Sea field data of a series of random wave and current computer models of bed boundary layer flows and associated suspended sediment concentrations. The EC-funded (MAST 1) work is part of a larger project, which also includes the laboratory testing of a new seabed shear stress meter (SSM) and the field collection of nearbed data using a special boundary layer rig (STABLE). Both two-dimensional (2DV) and one-dimensional (1DV) hydrodynamic models are described based on a mixing length closure but including simulation techniques to enable the inclusion of both long and short-crested random waves and steady currents. A 1DV suspended sediment model is also described with realistic boundary conditions to enable the simulation of vortex entrainment from seabed ripples. Application of the various models to the SSM and STABLE data shows realistic results.

1. INTRODUCTION

The present paper is concerned with the computer simulation of water and sediment movements over rippled seabeds in random wave and current conditions appropriate to the North Sea. It reports on one element of a larger multi-disciplinary research programme involving engineers, oceanographers and geologists, who are studying the formation of nearshore sandbanks and their role in providing protection to adjacent coastlines.

---

1. Department of Civil Engineering, University of Liverpool, L69 3BX, England.

2. Versuchsanstalt für Wasserbau und Schiffbau, Berlin, Germany.

3. Proudman Oceanographic Laboratory, Bidston Observatory, L34 7RA, England.

The research involves the field and laboratory testing of equipment to measure near-bed waves and currents and the associated sediment transport rates. In particular, staff from VWS, Berlin, have tested an improved seabed shear plate (SSM) to enable the direct measurement of seabed shear stress in waves and currents, Oebius (1992). Staff from the NERC's Proudman Oceanographic Laboratory have used a large bed boundary layer rig (STABLE) to provide field information on near-bed turbulence, waves, currents and sediment movements at the Brown Ridge Sandwave Site in the North Sea, Williams (1991). In addition, staff from the Department of Civil Engineering at Liverpool University have developed a series of hydrodynamic and sediment transport computer models to help with the interpretation of the data collected by both the SSM and STABLE rigs.

2. MODEL WORK

Four models have been developed: a two-dimensional (x, z) full-depth rough-turbulent hydrodynamic model (2DV) to study advective (mass-transport) effects on vertical mixing; a two-dimensional (x, z) bed boundary layer hydrodynamic model of wave-induced flow over bed ripples to assist with vortex entrainment ideas (2DV); a one-dimensional, rough-turbulent hydrodynamic model (1DV) to simulate wave-current interactions at arbitrary intersection angles in directional random waves; and an associated one-dimensional suspended sediment model (1DV) to study vertical sediment distributions in directional random waves and hence the effect of wave groupiness.

2.1. 2DV Hydrodynamic Model

The model solves simplified forms of the horizontal momentum and mass continuity equations for multi-frequency waves using a mixing length closure. The model equations are given as:-

$$\rho\partial u/\partial t + \rho u\partial u/\partial x + \rho w\partial u/\partial z + \partial p/\partial x = \partial \tau_{xz}/\partial z \qquad (1a)$$

$$\partial u/\partial x + \partial w/\partial z = 0 \qquad (1b)$$

where u and w are the phase-point-average turbulent-mean flow velocities in the horizontal (x) and vertical (z) cartesian co-ordinate directions, respectively; p is pressure; ρ is the fluid density; and τ_{xz} is the horizontal component of the Reynolds stresses.

The wave-induced boundary layer is assumed to be thin and the motion outside it is assumed to be irrotational so that the pressure gradient in equation (1a) can be approximated by the equation:-

$$-\partial p/\partial x = \rho \partial u_\infty/\partial t + \rho u_\infty \, \partial u_\infty/\partial x \qquad (2a)$$

$$\text{with} \quad u_\infty = \bar{u}_\infty + \sum_{i=1}^{m} u_i \cos(i\omega t - ikx + \phi_i) \qquad (2b)$$

where u_∞ is the wave-induced orbital velocity at the sea surface (mean water level); $\bar{u}_\infty$ is a wave-period-averaged steady velocity component; u_i are velocity amplitudes of the m Fourier frequency components making up the wave signal; ω is the wave frequency (= $2\pi/T$, T is the wave period); and k is the wave number (= $2\pi/L$, L is the wave length).

The Reynolds stress (τ_{xz}) is approximated by a simple mixing length expression ($\rho\kappa\partial u/\partial z$), where $\nu_t = \kappa^2 z^2 \partial u/\partial z$ and κ is Von Karman's constant (0.40).

The set of equations is solved using an implicit Crank-Nicolson finite difference technique on a space-staggered grid using zero velocity at the seabed ($z=z_o$), a zero velocity gradient at the water surface and repeating conditions for lateral boundaries, Kim (1993).

2.2. 1DV Hydrodynamic Model

The 1DV model also solves simplified flow equations using a mixing length closure. The model works for arbitrary-angled wave and current flows and uses simulation techniques involving surface wave spectra to produce appropriate model boundary conditions. The equations used in the model are given in tensor form as:-

$$\rho \partial u_i/\partial t - \partial p/\partial x_i = \partial \tau_{xzi}/\partial z \qquad (3a)$$

$$\partial p/\partial x_i = \rho \partial u_{\delta i}/\partial t + \rho g \partial H/\partial x_i \qquad (3b)$$

$$\tau_{xzi} = \rho \nu_t \partial u_i/\partial z; \quad \nu_t = \ell^2 \partial V/\partial z; \quad V = \sqrt{(u^2 + v^2)} \qquad (3c)$$

u_i (=u,v) are the cartesian velocity components in the horizontal (x) and lateral (y) co-ordinate directions respectively; x_i are the co-ordinates x, y respectively; g is the acceleration due to gravity; $\partial H/\partial x_i$ is the mean water surface slope; ℓ is a mixing length (=κz) and $u_{\delta i}$ are the u, v components at the top of the wave boundary layer, respectively.

Equation 3 can be solved in terms of a shear velocity (p_*, $\tau_{xz} = \rho p_*^2$) - see Bakker (1974), Wong (1984) for the case of co-linear waves and currents. Alternatively, the vertical co-ordinate (z) can be transformed by a power law and the transformed equations solved directly for u_i.

Both approaches have been used in the MAST 1 work. However the transformed co-ordinate approach is simpler to use for directional wave simulations. In this lattermost case the surface boundary conditions for the variation of velocity (U_T) with time is obtained from simulation techniques, see for example, Ellis et al (1981).

$$U_T = \sum_{m=1}^{M} \sum_{n=1}^{N} \left(\frac{2\pi f_m}{\sinh (k_m h)} \right) F \qquad (4a)$$

$$F = a_{m,n} \cos (2\pi f_m t + \phi_m) \cos\theta_n \qquad (4b)$$

where f_m is the wave frequency ($=1/T_m$, T_m is the wave period); ϕ_m are random phase angles in the range 0 - 2π; k_m is the wave number; h is the water depth; t is time; and $a_{m,n}$ is a wave amplitude obtained by integration of the directional wave energy spectrum. Thus:-

$$a_{m,n} = \sqrt{(2\, S(f_m, \theta_m)\, \Delta f_m . \Delta\theta_n)} \qquad (5a)$$

$$S(f_m, \theta_m) = S(f_m).\, G(f_m, \theta_n) \qquad (5b)$$

$$G(f_m, \theta_n) = G_0 \cos^{2s}(\theta_n/2) \qquad (5c)$$

$$G_0 = 2^{2s-1} . \Gamma^2 (s+1)/(\pi . \Gamma(2s+1)) \qquad (5d)$$

where G_0 is a constant dependent upon parameter s, which varies with peak spectral frequency and has a typical value of 20, Goda (1985); Γ is the Gamma function; θ_n is a wave direction in the range $\pm$ 90° of the dominant wave direction; $S(f_m, \theta_n)$ is any directional surface wave energy spectrum; $S(f_m)$ is a surface wave energy frequency spectrum; $G(f_m, \theta_n)$ is a spectral wave energy spreading function. $\Delta\theta_n$ is the band width of the n-th directional wave angle obtained by dividing the range of wave angles ($\pm$90°) into n equal intervals and Δf_m is the bandwidth of the m-th frequency interval obtained from the co-cumulative energy spectrum by using equal energy bands, see Ellis et al (1981).

A zero-velocity bed boundary condition is used (u=w=0) at $z=z_0$. The value of z_0 can be adjusted in random wave simulations using Madsen's (1990) approach, if desired.

2.3. 1DV Sediment model

In order to study the vertical distribution of suspended sediment over a rippled seabed, a one-dimensional sediment model has been used. The model equations used are:-

$$\partial c/\partial t + (\tilde{w} - w_f)\partial c/\partial z = \partial(\epsilon_s \partial c/\partial z)/\partial z \qquad (6)$$

where c is the phase-point-averaged turbulent-mean suspended sediment concentration; $\tilde{w}$ is the vertical wave induced fluid velocity; w_f is the effective vertical sediment diffusion coefficient.

Previous work has generally ignored the effect of $\tilde{w}$, and has determined ϵ_s during the wave cycle from the hydrodynamic shear stress determined by a 1DV-type model, see for example, Davies (1990). Such an approach does not include all the major processes contributing to vertical mixing, see for example, O'Connor (1991). The inclusion of extra mixing has usually been done in the past by taking a wave-period-average view of vertical sediment distributions and then using the sediment distribution itself to determine effective mixing coefficients see for example, Van Rijn (1989), In the MAST 1 work, a different approach has been used. Sediment is released into the water column at two discrete times during the wave period (at t = T/16 and 9T/16 for a mono-wave) at a height of between one and two ripple heights above the mean bed level, as suggested by the 2DV model tests for a rippled bed, see O'Connor et al (1992). Shear-induced entrainment is also allowed during the wave period as dictated by the 1DV hydrodynamic bed shear stress, see Figure 1. Additional mixing due to mass-transport is allowed by using the 2DV "flat"-bed hydrodynamic model (see Section 2.1) to provide the ϵ_s values.

Solution of equation (6) is achieved by a number of intermediate steps. Firstly, a transformed vertical co-ordinate is used in order to resolve the large near-bed concentration gradients. The same approach was used for the 1DV hydrodynamic equations. Secondly, a split operator finite difference approach is used to introduce the vortex entrainment concentrations into the water column at a height of 1.5 Δ_r above the mean bed level (z = 0). Thirdly, the new equations are then solved sequentially using appropriate boundary conditions between the water surface (mean see level) and the sea bed $z=z_o$; the co-ordinate origin being located half a ripple height above a ripple trough.

The necessary equations are given below:-

$$\partial c/\partial t - w_f \, \partial c/\partial z = \partial \, (\epsilon_s \, \partial c/\partial z)/\partial z \qquad (7a)$$

$$\partial c/\partial t + \tilde{w}\partial c/\partial z = S(t) \qquad (7b)$$

$$S(t) = M_v/(\Delta_r T_v), \text{ for } \Delta_r \le z \le 2\Delta r, \text{ and} \qquad (7c)$$

$$^{5T}/_{16} \le t \le {}^{3T}/_{8}, \text{ or } {}^{13T}/_{16} \le t \le {}^{7T}/_{8}$$

$$M_v = \int_o^{T/2} E_v \, dt \qquad (7d)$$

$$E_v = (1-\alpha)E_t \; ; \; E_t = A\,\Phi^{1.5} \; ; \; T_v = T/16 \qquad (7e)$$

$$\Phi = \tau_b(t)/((\rho_s-\rho)\; g\; D_{50}) \qquad (7f)$$

Where $\tau_b(t)$ is the bed ($z = 0$) shear stress from the 1DV model; ρ_s is the sediment density; g is the acceleration due to gravity; D_{50} is the 50% finer grain size of the bed sediment; A, α are model constants determined by field/laboratory tests.

Equation 7a is solved by an implicit finite difference method while equation 7b is solved as a second step using the method of characteristics. The model uses a zero flux condition ($\epsilon_s\, \partial c/\partial z = -w_f c$) at the water surface and a surface entrainment condition at the seabed ($\epsilon_s \partial c/\partial z = \alpha E_t$ at $z=z_o$). Values of ϵ_s are obtained from the 2DV hydrodynamic model.

3. MODEL APPLICATIONS

3.1. 1DV Hydrodynamic Model Tests

The ability of the 1DV model to reproduce conditions in mono-frequency waves was demonstrated using the oscillating tunnel data of Jonsson and Carlsen (1975), see Wong (1984). In addition, data from the VWS flume tests, Oebius (1992) were reproduced using a suitable plate roughness ($2D_{50}$) and scale factor, see Figure 2.

The ability of the Bakker version of the 1DV model to reproduce velocities near the top of the wave boundary layer (10 mm above the bed) with multi-frequency (3 components) waves, and waves and currents was demonstrated by using the small-scale flume data of Savell (1986), see Figures 3,4. Good agreement is apparent for maximum amplitude and phase. The velocity model's ability to reproduce long-crested random waves was tested for conditions approximated to those at the Brown Ridge Site ($h = 30m$; $z_o = 0.01$ m. Wave conditions were assumed to be described by a Pierson-Moskowitz (PM) spectrum with significant wave height of $H_s = 2.5m$ (wind speed = 11 m/s) and a peak energy period of $T_m = 8.1$ s. The PM spectrum was simulated by 60 frequency components and the velocity time series used to drive the model.

The accuracy of the simulation process can be judged by Figure 5, which shows a compassion between the PM spectrum and the model spectrum obtained by subjecting the model surface elevation time series to a Fast Fourier Transform (FFT) analysis.

Typical bed shear stresses and orbital velocities from the model at the top of the wave boundary layer are shown in Figure 6 for a typical 64s time interval. The random nature of the results is clearly seen as is also the phase shift over the depth of the boundary layer.

Figure 7 shows the root-mean-square (rms) and significant amplitudes of the wave-induced orbital velocities from a direct analysis of model time series for conditions at the Brown Ridge Site. These significant values can be directly compared with the results from the 1DV model operated with representative mono-frequency wave heights and wave periods -the 'design-wave' approach. Figure 8 shows the results for the mono-wave simulations using H_s, T_{max} and H_s, T_z. It is clear that the best comparison with the random wave model is obtained with H_s, T_{max} and not with the more traditional H_s, T_z combination.

The 1DV model was next used to investigate the effect of short-crested seas. The Brown Ridge model with its PM spectrum was re-run with a Goda spreading function, equation 5, s = 20. Figure 9 shows the u, v velocity components for a short length of record while Figure 10 shows the corresponding instantaneous wave direction vectors. The groupy nature of the wave signal is clearly seen as is also the lateral scattering effect of the short-crested sea. Such lateral movements will add significantly to the dispersal of both sediment and pollutant within the water volume. Similar results to the 1DV model have also been found with the STABLE data, see O'Connor et al (1992).

In order to examine the 1DV model's ability to reproduce the correct magnitude and phase of velocities within the boundary layer, use was made of S4 current meter data collected during the STABLE deployment at the Brown Ridge Site, see Williams (1991) Field velocities for a 22 second period at 800mm above the seabed were used as the upper boundary condition in the model. Figure 11 shows the comparison of field results at 800mm and 400mm with model results at 70mm. It is clear that the model reproduces the main features of the field results.

3.2. 1DV SEDIMENT MODEL APPLICATIONS

The ability of the 1DV model to reproduce suspended sediment concentrations during a wave period was tested using laboratory data of Bosman (1982). Figure 12 shows quite a good comparison considering the difficulty in obtaining such laboratory data.

The need for the inclusion of extra mixing in 1DV models is illustrated by the wave-period-average results of Figure 14. Both the 2DV and 1DV hydrodynamic models were used for conditions appropriate to Bosman's (1984) laboratory studies,

and the wave-period-average mixing coefficient (ϵ_s) determined by period-averaging. The 1DV sediment model was then used with vortex and shear-induced entrainment to reproduce wave-period-average concentrations, Figure 13. It is clear that the extra mixing inherent in the 2DV model is essential for correct simulation of sediment profiles.

Finally, the long-crested 1DV random wave model was used to simulate suspended sediment conditions at the Brown Ridge Site, see Figure 14. The influence of groupiness in the wave and shear records is clearly seen to influence suspended sediment concentrations with the larger groups having the greatest effects. Unfortunately, no comparable field data was obtained from the STABLE deployment and consequently, more field data is needed to test model ideas further.

4. CONCLUSIONS

A range of 1DV and 2DV bed boundary layer models have been developed to assist with interpretation of field data obtained from the Brown Ridge Sandwave Site in the Southern North Sea. Comparison of model results with mono-and multi-frequency laboratory data for both velocities and shear stresses shows good results. Realistic model simulations were also obtained for both long and short-crested random wave conditions when compared with measured field data. Use of the long-crested 1DV hydrodynamic model also demonstrates the importance of using the correct wave period when using the mono-frequency "design wave" approach to predict seabed velocities and shear stresses.

An 1DV suspended sediment model was also developed with new boundary conditions which attempted to reproduce the influence of both vortex and shear-induced entrainment. Good comparisons were obtained with laboratory data. The importance of including enhanced mixing due to mass-transport currents in 1DV model simulations was also demonstrated as was the influence of wave groupiness on sediment concentrations at the Brown Ridge Field Site.

5. ACKNOWLEDGEMENTS

The authors are grateful for financial assistance from the Commission of the European Directorate General for Science, Research and Development under Contract No. MAST - 0036(C).

References

Bakker, W.T., (1974). Sand Concentration in an Oscillatory Flow. Proc. 14th Coastal Eng. Conf. ASCE, pp 1129-1148.

Bosman, J.J., (1982). Concentration Measurements under Oscillatory Water Motion. Delft Hydraulics Laboratory/TOW Report on Model Investigation M1695 Part II. Delft.

Bosman, J.J. (1984). Design and Specification of OPCON, on Optical Instrument for Instantaneous Sediment Concentration Measurements. Report on Investigation R716, Part VI, Delft Hydraulics Laboratory.

Davies, A.C., (1990). Modelling the Vertical Distribution of Suspended Sediment in Combined Wave-Current Flow. Proc. 5th Int. Conf. on the Physics of Estuaries and Coastal Seas. (In Press).

Ellis, C.P., O'Connor, B.A. and McDowell, D.M., (1981). Ceneration of Laboratory Waves using a Microcomputer. 2nd Int. Conf. on Engineering Software, Imperial College, London, pp 899-913.

Coda. Y., (1985). Random Seas and Design of Maritime Structures. University of Tokyo Press, 323 pp.

Jonsson, I.C. and Carlsen, N.A., (1975). Experimental and Theoretical Investigations in an Osillatory Turbulent Boundary Layer. J. Hydr. Res., Vol. 14, No. 1, pp 45-60.

Kim, H., (1993). A Three Dimensional Sediment Transport Model. Ph.D. Thesis, Dept. of Civil Engineering, University of Liverpool (in preparation).

Madsen, O.S., Mathison, P.P. and Rosengaus, M.M., (1990). Moveable Bed Friction Factors for Spectral Waves. Proc. 22nd Coastal Eng. Conf., ASCE, pp 420-429.

O'Connor, B.A., (1991). Suspended Sediment Transport in the Coastal Zone, Keynote Lecture, IAHR Symposium, Florence, 2-5 September, 1991, pp 17-63.

O'Connor, B.A., Williams, J.J., Oebius, H.U. and Sarmento A., (1992). Circulation and Sediment Transport on Sand Banks in European Shelf Seas. Final Report to DCXII, EC MAST Programme. Dept. of Civil Engineering, University of Liverpool.

Oebius, H.U., (1992). Circulation and Sediment Transport on Sand-Banks in European Shelf Seas. Part: Development of a Shear Stress Meter. Report No. 1208/92, VWS, Berlin, 100pp.

Savell, I.A., (1986). An Experimental Study of Near-Bed Hydrodynamics of Waves and Steady Current and the Effect of this on Sediment Transport. Ph.D. Thesis. Dept. of Civil Engineering, University of Manchester.

Williams, J.J., (1991). Wave, Current and Sediment Interaction Study. POL Cruise Report No. 13, RRS Challenge 87, 4-20 Dec. 1991, 30pp

Wong, Y.K., (1984). A Numerical Model for the Interaction of Combined Wave and Current Boundary Layers. M.Sc. Thesis, Dept. of Civil Engineering, University of Manchester.

Van Rijn, L.C., (1989). Handbook Sediment Transport by Currents and Waves. Delft Hydraulics, Report H461.

Figures

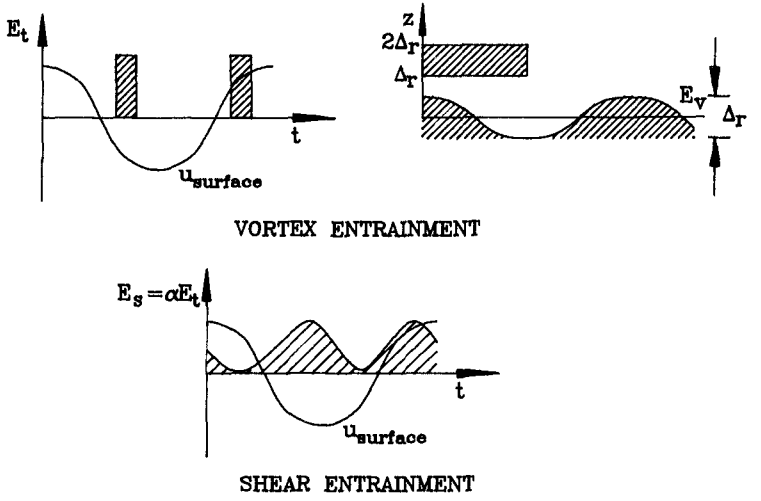

FIGURE 1

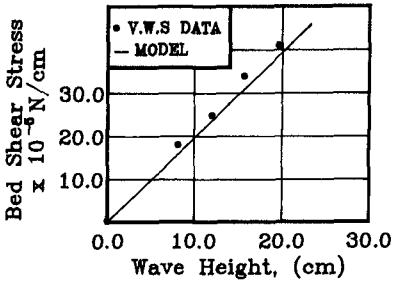

FIGURE 2

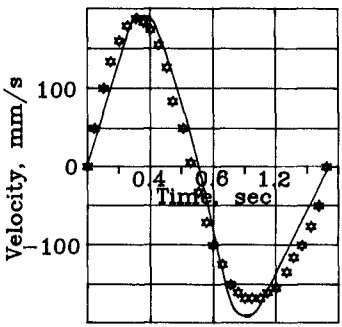

FIGURE 3

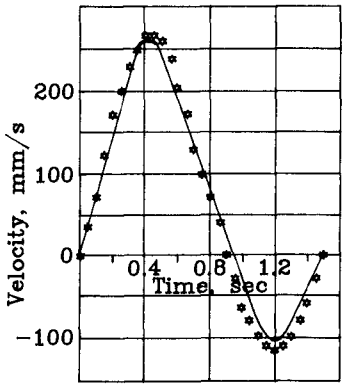

FIGURE 4

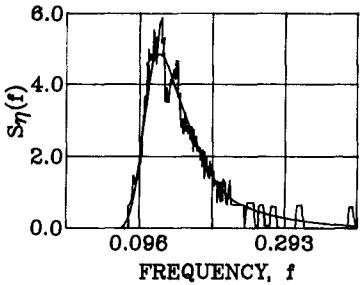

FIGURE 5

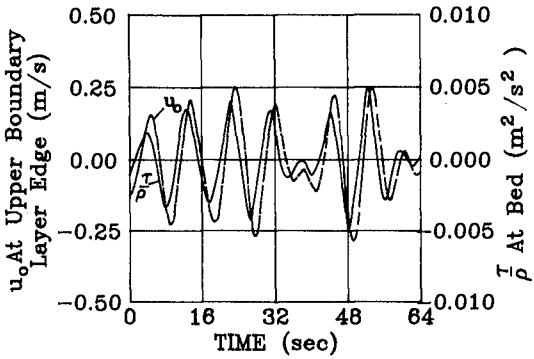

FIGURE 6

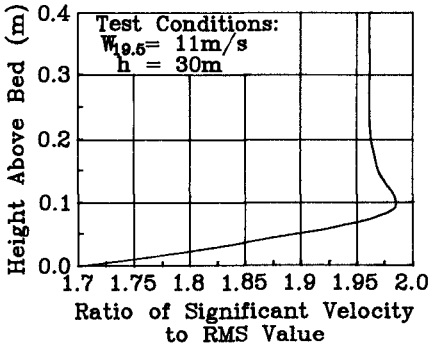

FIGURE 7

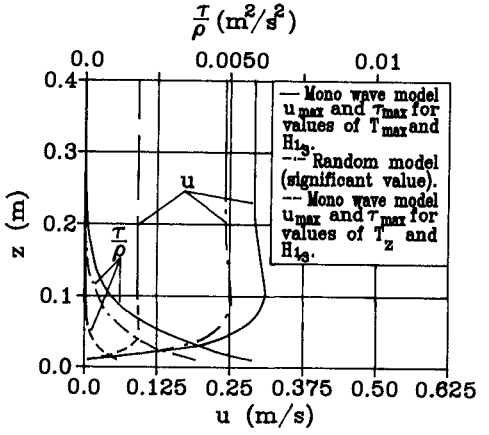

FIGURE 8

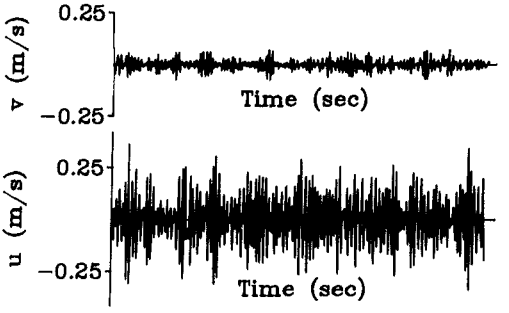

FIGURE 9

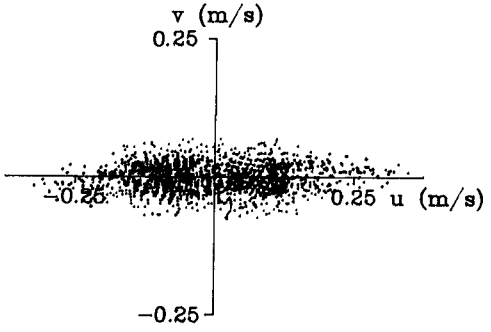

FIGURE 10

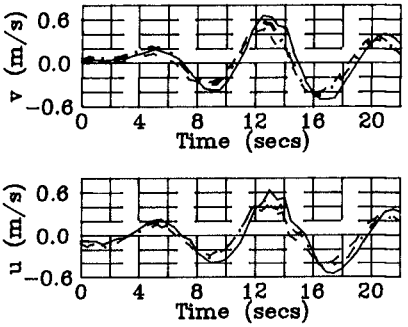

LEGEND:
Model/Field ——
(at 80cm above bed).
Field — —
(at 40cm above bed).
Model — - —
(at 7cm above bed).

FIGURE 11

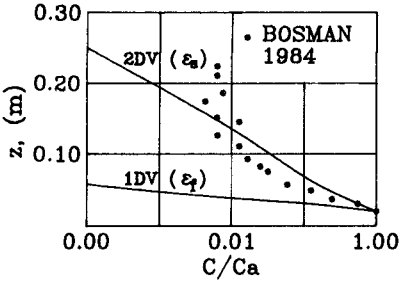

FIGURE 13

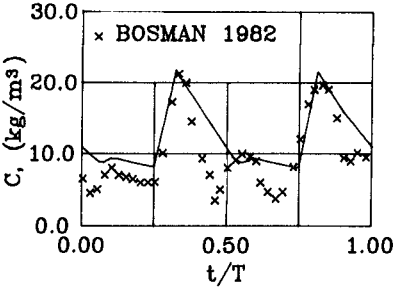

FIGURE 12

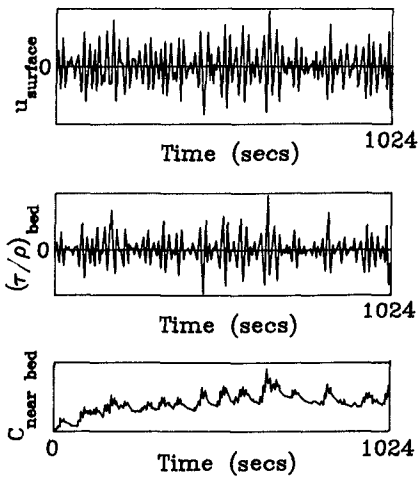
$u_{surface}$
0
Time (secs)
1024
$(\tau/\rho)_{bed}$
0
Time (secs)
1024
$C_{near\ bed}$
0
Time (secs)
1024

FIGURE 14